Excitons properties and quantum confinement in CdS/ZnS core/shell quantum dots

GUOZHI JIA[*]

Tianjin Institute of Urban Construction, Tianjin 300384, China

We investigate the electronic structures and quantum confinement of CdS/ZnS core/shell quantum dots by using the effective-mass approximation theory, taking account of the Coulomb interaction between the electron and hole. The calculated results shows that the electron and hole can be mainly localized in the core area for the CdS/ZnS type- Ⅰ heterostructure. The transition energies can be widely tuned by changing the structure parameters. The electron and hole wavefunctions are almost localized in the core area and there was a large overlap for the CdS/ZnS quantum dots. The changing of the 1s-1s transition energy in quantum dots with the changing core size are different dramatically from that with the changing shell size due to quantum size effects.

1. Introduction

Complex quantum structures have recently attracted a great deal of attention due to its potential application in light-emitting devices [1], biological tagging materials [2] and the solar cell [3]. Modern colloidal techniques are allowed to fabricate different kinds of highly luminescent quantum dots (QDs) via organometallic routes [2,4] or aqueous method [5]. One can also grow the composite semiconductor structure by combining different materials to improve the emission quantum yields [5] or spatially separate electrons and holes in the different parts of nano-particles [6-9] for specific application. Quantum confinement of carriers can remarkably modify the physical properties of materials. These features has attracted many researchers to develop the optical characterization of QDs.

The effective mass and confinement potential energy play critical roles in the carriers distribution in the core/shell QDs. The confinement potential energies of carriers mainly depend on the core radius, shell size and the ratio between core and shell. The different structures are designed to achieve the separation of the carriers spatial distribution. Haus *et al.* applied the effective mass approximation to calculate the electronic structure of Quantum-dot quantum well (QDQW). They systematically investigated the electron and hole wave functions, the 1*s* transition energy, and the overlap of the wave functions [10]. Schooss *et al.* further took into account the Coulomb interaction between electron and hole, the results showed that the probabilities of the carriers could present in the different layers in the QDQW CdS/HgS/CdS structure [11]. Chang *et al.* pointed out that the spatially separated characteristic of

electron and hole could be enhanced significantly in QDQW with the two wells [12]. More recently, Nizamoglu *et al.* presented that the multi-color spontaneous emission might be obtained by the exciton localization in distinct layers in the onion-like QDQW structure [13]. It is therefore of great interest and importance to engineer spatial distributions wave function of electron and hole in nano-particles [6].

To date, CdS/ZnS core-shell QDs [14,15] and ZnS/CdS/ZnS QDQW core/shell/shell structure [16,17] have been synthesized and shown promising application in efficient green-blue light emitting. The lattice parameter of ZnS with a blende type (a=5.406Å) is close to that of CdS (a=5.818Å), which can be expected to exhibit well CdS/ZnS core/shell growth due to the small lattice mismatch (6.4%). Although both the valence and conduction bands of the CdS core are lower than those of the ZnS shell, the hole is weakly confined in CdS core due to the valence band offset which is only 0.2eV [6]. Therefore, it is essential to theoretically analyze the excitons distribution in the CdS/ZnS core/shell structure to understand the physics for improving the QDs performance.

In this letter, we investigate electron and hole wave function behaviors in CdS/ZnS core/shell structure nanocrystals with the changing of the core radius and the shell thickness. The mechanism of the excitons spatial distribution is discussed, in which is mainly attributed to the effect of valence band offset on carrier quantum confinement for different structure QDs.

2. Theory

We consider the core/shell structure QDs, which

consisted of ZnS shell and CdS core materials. When the space-dependent effective mass of carriers is taken into account, the Schrodinger equation of carriers in the framework of the effective mass approximation in the QDs region is as follows:

$$\left(-\frac{\hbar^2}{2}\nabla\frac{1}{m_i}\nabla - V(r) \right)\Psi(r) = E\Psi(r) \qquad (1)$$

where $\hbar$ is Planck's constant divided by 2π, m_i and $V(r)$ the particle mass and a potential depending on the position in the QDs, E the energy eigenvalue, and $\psi(r)$ the corresponding eigenfunction. Here, we consider QDs as spherically symmetric structure and having homogeneous potentials, which make the wave functions be separated into the radial and angular parts as follows:

$$\Psi_{nlm}(r,\theta,\phi) = R_{nl}(r)Y_{lm}(\theta,\phi) \qquad (2)$$

$R_{nl}(r)$ is the radial wave function, and $Y_{lm}(\theta,\phi)$ a spherical harmonic. n is the principal quantum number, and l and m are the angular momentum numbers. We shall restrict the calculations to 1s states for $n=1$, $l=m=0$. We obtain the solutions for QDs by solving the continuity relations of the carriers wave functions and the probability currents at the boundaries:

$$R_{nl,i}(k_i r_i) = R_{nl,i+1}(k_{i+1} r_i) \qquad (3)$$

$$\frac{1}{m_i}\frac{dR_{nl,i}(k_i r_i)}{dr}\bigg|_{r=r_i} = \frac{1}{m_{i+1}}\frac{dR_{nl,i+1}(k_{i+1} r_i)}{dr}\bigg|_{r=r_i} \qquad (4)$$

where $k_{i/i+1} = \left[\dfrac{2m_i(E-V)}{\hbar^2}\right]^{1/2}$ is the wave vectors in core and shell, respectively, $R_{nl,i}(r_i)$ and $R_{nl,i+1}(r_i)$ are the radial wave functions for the carriers (electron or hole) in the core and shell, respectively, m_i and m_{i+1} are the carrier effective masses in the CdS and ZnS, respectively. For simplicity, we assume that the QDs was placed in a infinite potential well. That is to say, no wave functions tunnel from the QDs to the outside of QDs with taking into account the complete confinement. Thus, at

the outer boundary of the QDs, the nontrivial solution can be obtained to determine the general energy eigenvalues by letting the determinant of the coefficients of the wavefunction at the interface as zero.

The Coulomb interaction energy between electron and hole pair can be treated as a heliumlike perturbation according to the first-order perturbation approximation. After expanding of $1/|r_e - r_h|$ in spherical harmonics form and integrating the angular coordinates, the Coulomb interaction energy can be expressed as [11,13]

$$E_c = -\frac{e^2}{4\pi\varepsilon_0}\iint dr_e dr_h r_e^2 r_h^2 \frac{|R_e(r_e)|^2 |R_h(r_h)|^2}{\max(r_e,r_h)\bar{\varepsilon}(r_e,r_h)} \qquad (5)$$

The schematic energy diagram of the CdS/ZnS core/shell under investigation is shown in Fig. 1. From the diagram, it can be inferred that ZnS has the higher valence and conduction bands than CdS, which corresponds to the classic Type-Ⅰ semiconductor heterostructure.
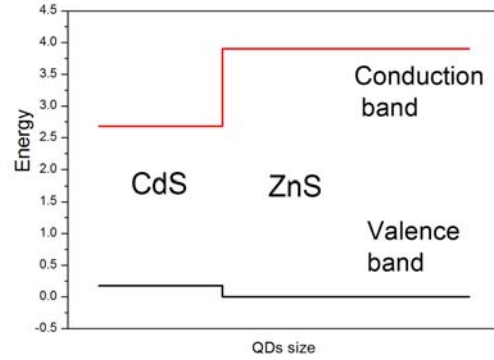

Fig. 1. Potential energies for the electron and hole in CdS/ZnS QDs structure.

3. Results and discussion

To investigate the influence of structure parameters (core radius r and shell thicknesses R) on spatial distributions of carriers, we performed the radial probabilities of the carriers in the lowest energy 1s eigenstates for CdS/ZnS core/shell QDs. The values of the physical parameters used in our calculations are given in Table 1. Fig. 2 shows the radial probabilities of electron and hole with different ZnS shell thickness. It can be seen that the wave function of the electron can slightly spread out the CdS core with the increasing of ZnS shell thickness. It is also found that the shell thickness weakly affects the probability of hole at the core of the QDs, and the probability of electron are insensitive to the shell thickness at the core area. As for 0.5 nm shell thickness, both of the electron and hole are completely localized at the range of core. When the shell

thickness increases continuously, the electron and the hole can mainly be confined in the core, since the hole haven't enough energy across the barrier for the energy band offset in valence band (1.22eV) and in conduction band (0.18eV) [18]. The lowest energy level of the hole is increasing gradually, but the carriers don't exceed the confinement ability of the barrier height with the increasing of the shell thickness due to the quantum confinement effect.

Table 1. Material parameters for CdS and ZnS.

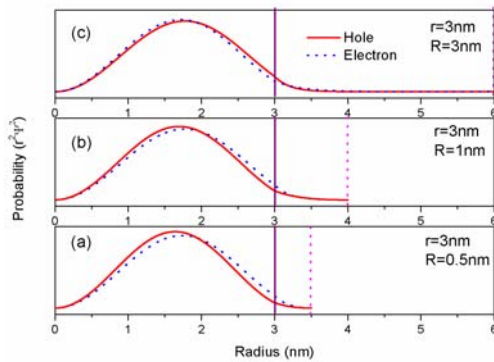| Material	m_e/m_0	m_h/m_0	Dielectric constants	Band gap (eV)
CdS [10]	0.2	0.7	5.5	2.5
ZnS [10]	0.28	0.410	8.10	3.10

Fig. 2. The probability of the presence of electron and holes in the lowest energy 1s eigenstates in CdS/ZnS QDs structure with the different shell thickness   R and keeping the core diameter constant r=3 nm.

Fig. 3 shows the variation of the 1s-1s transition energy (a), the Coulomb interaction energy (b), and the overlap integral (c) versus the shell thickness with the core diameter fixed. It can be seen that the 1s-1s transition energy has changed only about 0.08 eV with the variation of the shell size, which implies the slight effect of the confinement potential on the transition energy with the increasing of the shell thickness. The Coulomb interaction energy strongly depends on the shell size when the shell size is less than 1.5 nm, which can be attributed to the confinement of carriers enhanced for the thin shell thickness due to the influence of the outer infinite potential. Interestingly, the overlap integral increases with the slight increasing of the shell size, indicating the carriers are localized in the area of core. It is well known that the carriers are localized in the shell or core region, determined by the effective masses and the energy band offsets between the core and shell materials. For thick ZnS

shells (＜1.5 nm), the outer infinite potential play an important role in confining the carriers in the core region. As the shell thickness increases, the confinement of carriers is increased.
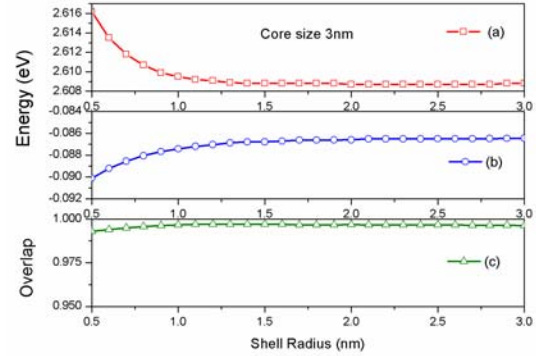

Fig. 3. The calculation of the 1s-1s transition energy (a), the Coulomb interaction energy (b), and the overlap integral (c) as   a function of the shell size with the core diameter fixed (r=3 nm).

There are very different results from that of the carriers distribution in the QDs with variation of the core radius when the shell size is fixed. Here, the shell thickness was fixed at 3 nm, the core radius was varied from 0.5 to 3 nm. As shown in Fig. 4, the probabilities of the hole are independent on the core radius for the thick shell R=3 nm, and the hole is primarily localized in the shell.
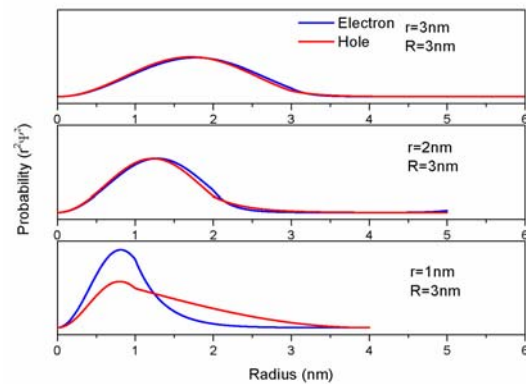

Fig. 4. The probability of the presence of electron and holes in the lowest energy 1s eigenstates in CdS/ZnS QDs   structure with the different   core diameter r and keeping the shell size constant R=3nm.

For the core radius of 1nm, the electron can obtain sufficient kinetic energy to span the conduction potential barrier in the interface between the core and shell, and is located at the entire QDs region. In the shell layer, the probability of the hole decreases with the increasing of

the core radius. Unfortunately, the electron probability in the interface is very large, which is likely attributed to the increasing of the nonradiative recombination probability between the interface defects and the holes [8, 11]. When the core radius increases to 2 nm, the electron and hole are distinctly localized in the core area. As the core radius further increases, the electron and hole wavefunctions are almost completely localized in the core area and remain an small probability in the interface of heterostructure.

In Fig. 5, we plot the 1s-1s transition energy (a), the Coulomb interaction energy (b), and the overlap integral (c) as a function of the core radius with the shell thickness fixed. It is worth noting that the emission wavelength can be tuned among a very wide range. Compared with the results in Fig. 3(a), the variation of core size can be considerably more effective in tuning the emission wavelength than the changing of the shell thickness. As shown in Fig. 5(c), the overlap integral rapidly decreases as the core radius increases from 0.5 nm to 0.8 nm, and the overlap integral increases to 1 as the core radius is 1.5 nm. When the core radius is larger than 1.5 nm, the electron and hole are completely localized in the same area. Note that the Coulomb interaction energy first decreases and then slightly increases. This arises from the variation of the electron and hole probability at the interface between the core and shell with the ratio of core and shell size.
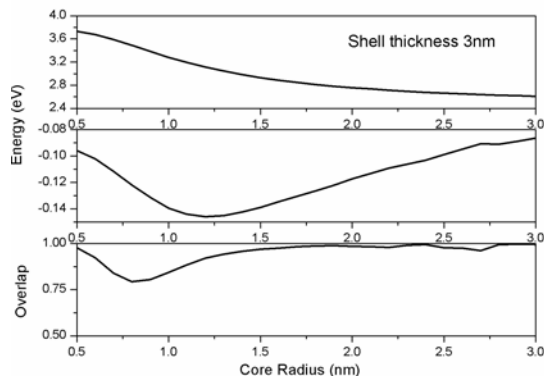

Fig. 5. The calculation of the 1s-1s transition energy (a), the Coulomb interaction energy (b), and the overlap integral (c) as a   function of the core diameter with the shell size fixed (R=3 nm).

4. Conclusions

In general, we study the electronic structures of CdS/ZnS core/shell structure QDs, including the Coulomb interaction between electron and hole. It is found that the 1*s* transition energies depend sensitively on the core radius of the QDs, while weakly on the shell size and the ratio of core and shell size. The electron and hole wavefunctions are almost completely localized in the core area and remain a large overlap for the CdS/ZnS quantum dots. The quantum confinement plays an important role in the transition energies and overlap integral of the carriers. Further work will focus on the effect of QDs structure and carriers distribution on the fluorescence efficiency of QDs.

References

[1] S. Y. Ryu, B. H. Hwang, K. W. Park, H. S. Hwang, J. W. Sung, H. K. Baik, H. O. Lee, S. Y. Song, J. Y. Lee, Nanotechnology **20**(6), 065204 (2009).
[2] X. H. Gao, Y. Y. Cui, R. M. Levenson, L. W. K. Chung, S. M. Nie, Nat Biotechnol **22**, 969 (2004).
[3] S. Y. Jin, T. Q. Lian, Nano Letters **9**(6), 2448 (2009).
[4] L. H. Qu, X. G. Peng, J. Am. Chem. Soc. **124**(9), 2049 (2002).
[5] Y. He, H. T. Lu, L. M. Sai, Y. Y. Su, M. Hu, C. H. Fan, W. Huang, L. H. Wang Adv. Mater. **20**(18), 3416 (2008).
[6] L. P. Balet, S. A. Ivanov, A. Piryatinski, M. Achermann, V. I. Klimov, Nano Letters **4**(8), 1485 (2004).
[7] S. J. Kim, B. Fisher, H. J. Eisler, M. Bawendi, J. Am. Chem. Soc. **125**(38), 11466 (2003).
[8] S. A. Ivanov, A. Piryatinski, J. Nanda, S. Tretiak, K. R. Zavadil, W. O. Wallace, D. Werder, V. I. Klimov, J. Am. Chem. Soc. **129**, 11708 (2007).
[9] G. Z. Jia, X. N. Fei, J. Wang, Chalcogenide Letters **7**(3), 181 (2010).
[10] J. W. Haus, H. S. Zhou, I. Honma, H. Komiyama, Physical Review B **47**(3), 1359(1993).
[11] D. Schooss, A. Mews, A. Eychmuller, H. Weller, Phys. Rev. B **49**(24), 17072 (1994).
[12] K. Chang, J. B. Xia, Physical Review B **57**(16), 10780 (1998).
[13] S. Nizamoglu, H. V. Demir, Optics Express **16**(6), 3515 (2008).
[14] J. S. Steckel, J. P. Zimmer, S. Coe-Sullivan, N. E. Stott, V. Bulović, M. G. Bawendi, Angew. Chem. Int. Ed. **43**(16), 2154 (2004).
[15] V. T. K. Lien, C. V. Ha, L. T. Ha, N. N. Dat, J. Phys.: Conf. Ser. **187**(1), 012028 (2009).
[16] L. X. Cao, S. H. Huang, S. Z. Lü, J. L. Lin, Journal of Colloid and Interface Sciences **284**(2), 516 (2005).
[17] L. X. Cao, S. H. Huang, S. L. E, Journal of Colloid and Interface Sciences **273**(2), 478 (2004).
[18] S. H. Wei, A. Zunger, Appl. Phys. Lett. **72**(16), 2011 (1998).

*Corresponding author: dip-coating@163.com